INTERNATIONAL JOURNAL FOR NUMERICAL AND ANALYTICAL METHODS IN GEOMECHANICS
Int. J. Numer. Anal. Meth. Geomech., **23**, 355–374 (1999)

FINITE ELEMENT ANALYSIS OF CONSOLIDATION OF LAYERED CLAY SOILS USING AN ELASTIC VISCO-PLASTIC MODEL

GUOFU ZHU AND JIAN-HUA YIN*

Department of Civil and Structural Engineering, The Hong Kong Polytechnic University, Hung Hom, Kowloon, Hong Kong

SUMMARY

This paper presents a general one-dimensional (1-D) finite element (FE) procedure for a highly non-linear 1-D elastic visco-plastic (1-D EVP) model proposed by Yin and Graham[1,2] for consolidation analysis of layered clay soils. In formulating the 1-D FE procedure, a trapezoidal formula is used to avoid the unsymmetry of the stiffness matrix for a Newton (modified Newton) iteration scheme. Unlike many other 1-D FE approaches in which the initial *in situ* stresses (or stress/strain states) are considered indirectly or even not considered, the initial *in situ* stress/strain states are taken into account directly in this paper. The proposed FE procedure is used for analysis of 1-D consolidation of a clay with published test results in the literature. The FE modelling results are in good agreement with the measured results. The FE model and procedure is then used to analyse the consolidation of a multi-layered clay soils with a parametric study on the effects of the variations of creep parameters in Yin and Graham's 1-D EVP model. It is found that the creep parameters ψ/V and t_0 have significant influence on the compression and porewater pressure dissipation. For some boundary conditions, changes of parameters in one layer will have some effects on the consolidation behaviour of another layer due to the different consolidation rates. Finally, the importance of initial stress/strain states is illustrated and discussed.

Key words: consolidation; creep; elastic visco-plastic; finite element modelling; compression; porewater pressure

INTRODUCTION

The consolidation analysis of clay strata, such as the prediction of settlement of foundation and reclamation over clay soils is of practical importance in geotechnical engineering. The first rational approach to this problem based on the principle of effective stress was proposed by Terzaghi.[3] Since then, extensive research has been carried out in this field. A logical extension of Terzaghi's one-dimensional consolidation theory to three-dimensional situation is due to Biot's fully coupled poroelastic formulation.[4] However, both Terzaghi and Biot's theories assume that the soil behaviour is linear elastic. The stress–strain behaviour is normally consolidated clay has

*Correspondence to: Professor Jian-Hua Yin, Department of Civil and Structural Engineering, The Hong Kong Polytechnic University, Hung Hom, Kowloon, Hong Kong

Contract grant sponsor: The Hong Kong Polytechnic University
Contract grant sponsor: UGC (Grant No. pdyU 63/96E) of Hong Kong SAR Government of China

CCC 0363–9061/99/040355–20$17.50

Received 20 May 1997
Revised 21 April 1998

been clearly demonstrated to be elastoplastic and viscous in nature.[5] Some models accounting for creep behaviour have been put forward.[1,2,6–11] Because of the complexity of the coupled set of partial differential equations, analytical solutions can only be found in limited cases. For general situations, most researchers resort to numerical techniques. Schiffman and Arya,[12] on the basis of Terzaghi's one-dimensional (1-D) consolidation model, investigated soil consolidation by finite difference method and finite element method. Desai *et al.*[13] suggested a non-linear soil model and implemented this model in 1-D consolidation analysis by finite elements. The 1-D consolidation analysis using elastic visco-plastic soil models was carried out by Garlanger,[14] Kabbaj *et al.*[15] and Yin and Graham[16] among others by finite difference method. However, few people conducted the consolidation analysis of field problems taking into consideration of (a) the time-dependent behaviour of soils, (b) variation of loading, and (c) multi-layers.[13,17]

It is well known that the time-dependent settlement of a clay layer is due to (a) hydrodynamic time lag and (b) the creep nature of the soil skeleton. One particular aspect of the 1-D consolidation behaviour that has consistently attracted attention is the 'primary' and 'secondary' consolidation behaviour. This raises the question of whether creep effects must be accommodated in the analysis of 'primary' compression or can be ignored until excess porewater pressures have largely dissipated. Two different approaches exist in this regard (here called Hypothesis A and Hypothesis B). In Hypothesis A[18,19] primary consolidation strains associated with transferring pore water pressures into effective stresses are separated from secondary consolidation strains arising from viscous deformations. Terzaghi's consolidation theory is used to calculate the compression at the end of primary consolidation, and a separate coefficient of secondary consolidation is then used to calculate the creep settlement. Hypothesis B assumes that creep occurs during and after the primary consolidation process. Recently, a new elastic visco-plastic model (EVP) for 1-D straining has been developed by Yin and Graham[1,2] based on the idea of 'equivalent time'. Yin and Graham's model has been verified for a number of soils and applied in a simple 1-D consolidation analysis under a constant loading condition by finite difference method.[1,2,16] The approach used by Yin and Graham[16] and the FE modelling in this paper conform with Hypothesis B.

Although field problems are three dimensional in nature, application of the two- and three-dimensional procedure[20–24] to include elastic plastic and time-dependent behaviour of soil may not be simple, and can be expensive. The 1-D straining approach can be applied to a number of problems where the situations can be approximated as one-dimensional. In addition, the importance of this approach to geotechnical engineering practice is attested by the fact that the settlement estimation of foundations on cohesive soils is based largely on 1-D straining model. This paper derives the formulation of a 1-D finite element procedure with emphasize on implementation of a highly non-linear EVP model for the time-dependent behaviour of soils. This 1-D FE procedure is used to analyse the consolidation of clay layers. The effects of the variations of creep parameters and initial stress/strain states are investigated.

GOVERNING EQUATIONS OF CONSOLIDATION PROBLEMS

The partial differential equations governing 1-D consolidation problems are first presented. It is assumed that (a) the soil is fully saturated, (b) water and soil particles are incompressible, (c) Darcy's law is valid, (d) compression and flow are one-dimensional (vertical), and (e) strains are small. A finite element (FE) model based on the governing equations is developed in the following section for simulating the consolidation of layered soils.

(a) The continuity equation

$$\frac{\partial q}{\partial z} = \frac{\partial \varepsilon}{\partial t} \tag{1}$$

where q is the vertical flow rate, ε the vertical strain (positive for compression), z the vertical co-ordinate, and t the time.

(b) The constitutive equations

$$\frac{\partial \varepsilon}{\partial t} = \frac{\partial f(\sigma')}{\partial t} + g(\sigma', \varepsilon) \tag{2}$$

Many 1-D models can be expressed in the form of equation (2), and $f(\sigma')$ and $g(\sigma', \varepsilon)$ may be different for loading and unloading for some models. For Terzaghi's model

$$\begin{aligned} f &= m_v \sigma' \\ g &= 0 \end{aligned} \tag{3}$$

where m is the soil compressibility and σ' the vertical effective stress.

For the non-linear elastic model used in this paper

$$\begin{aligned} f &= a \ln \sigma' \\ g &= 0 \end{aligned} \tag{4}$$

where a is a constant.

For Hardin's model[25]

$$\begin{aligned} f &= -\frac{1}{a + b\sigma'^{p}} \\ g &= 0 \end{aligned} \tag{5}$$

where a, b and p are constants.

For the 1-D elastic visco-plastic (EVP) model proposed by Yin and Graham[1,2]

$$\begin{aligned} f &= \frac{\kappa}{V} \ln \sigma' \\ g &= \frac{\psi}{V t_0} \exp\left(-\varepsilon \frac{V}{\psi}\right) \left(\frac{\sigma'}{\sigma'_0}\right)^{\lambda/\psi} \end{aligned} \tag{6}$$

where κ/V is a constant for elastic behaviour (V is specific volume), λ/V is a constant for the slope of a 'reference time' line (similar to the normally consolidated compression line, in other words, the virgin compression line), ψ/V is a creep parameter (similar to the 'secondary' consolidation coefficient, but defined differently), t_0 is a creep parameter in unit of time, σ'_0 is a constant parameter in unit of stress locating the 'reference time' line with $\varepsilon = 0$. Readers may refer to Yin and Graham[1,2] for more details about the derivation of equation (6) using 'equivalent time' concept, the definition and determination of model parameters and verification of the EVP model. The same name of parameters κ/V and λ/V are used in the Cam–Clay model for modelling the unloading/reloading behaviour and the normally consolidated behaviour of clays under isotropic loading.

(c) The Darcy's law

$$q = -k\frac{\partial h}{\partial z} \tag{7}$$

where k is the permeability and h the total water head.

Using the excess porewater pressure u, the Darcy's law becomes

$$q = -\frac{k}{\gamma_w}\frac{\partial u}{\partial z} \tag{8}$$

Equations (1), (2) and (8) are the governing equations for consolidation problems.

FINITE ELEMENT FORMULATION

The numerical solution of the consolidation model for a given boundary value problem is obtained here by using a Galerkin-type finite element weak formulation for the space variable z, coupled with a finite difference time scheme. Let the soil mass (domain Ω) be divided into a number of elements, with nodal points at the boundaries of each element. For an element Ω_e, the nodal points are denoted as z_m, z_{m+1} and the thickness h_e of the element is $z_{m+1} - z_m$.

Multiplying equation (1) by a virtual function $\phi(z)$, and integrating it, we have

$$\pi = \int_\Omega \phi\left(\frac{\partial q}{\partial z} - \frac{\partial \varepsilon}{\partial t}\right)\mathrm{d}z = \sum_{\Omega_e}\int_{\Omega_e}\left[\frac{k}{\gamma_w}\frac{\partial u}{\partial z}\frac{\partial \phi}{\partial z}\mathrm{d}z - \phi\left(\frac{\partial f}{\partial t} + g\right)\right]\mathrm{d}z + \phi q\Big|_{\Omega_b} = 0 \tag{9}$$

where Ω_b stands for the boundary. Equations (2) and (8) are used in deriving equation (9).

We do not follow the standard finite element approach to calculate the term $\int_{\Omega_e}\phi(\partial f/\partial t + g)\,\mathrm{d}z$ in equation (9). Otherwise an unsymmetric stiffness matrix will be obtained. In this paper, this term is simply integrated using the trapezoidal formula with the same error, that is,

$$\int_{\Omega_e}\phi\left(\frac{\partial f}{\partial t} + g\right)\mathrm{d}z = \frac{h_e}{2}(\phi_m, \phi_{m+1})\begin{bmatrix}\left(\dfrac{\partial f}{\partial t} + g\right)_m \\ \left(\dfrac{\partial f}{\partial t} + g\right)_{m+1}\end{bmatrix} \tag{10}$$

where the subscripts m and $m+1$ denote values at z_m and z_{m+1}, respectively.

Suppose ϕ and u are linear in every element Ω_e, then

$$\begin{aligned} u &= \mathbf{N}u_e \\ \phi &= \mathbf{N}\phi_e \end{aligned} \tag{11}$$

where $\mathbf{N} = (N_1, N_2)$, are the linear shape functions, $\phi_e = (\phi_m, \phi_{m+1})^{\mathrm{T}}$, $u_e = (u_m, u_{m+1})^{\mathrm{T}}$.

Substituting equations (10) and (11) into equation (9), we get

$$\pi = \sum_{\Omega_e}\phi_e^{\mathrm{T}}\left\{\frac{k}{\gamma_w h_e}\begin{bmatrix}1 & -1 \\ -1 & 1\end{bmatrix}u_e - \frac{h_e}{2}\begin{bmatrix}\left(\dfrac{\partial f}{\partial t} + g\right)_m \\ \left(\dfrac{\partial f}{\partial t} + g\right)_{m+1}\end{bmatrix}\right\} + \phi q\Big|_{\Omega_b} = 0 \tag{12}$$

Integrating equation (12) with respect to time from t_i to t_{i+1} using the generalized trapezoidal formula, we obtain

$$\pi = \sum_{\Omega_e} \phi_e^{\mathrm{T}} \left\{ \frac{k}{\gamma_w h_e} \begin{bmatrix} 1 & -1 \\ -1 & 1 \end{bmatrix} [\theta u_e^{i+1} + (1-\theta) u_e^i] \right.$$

$$\left. - \frac{h_e}{2} \begin{bmatrix} f_m^{i+1} - f_m^i + [\theta g_m^{i+1} + (1-\theta) g_m^i] \Delta t \\ f_{m+1}^{i+1} - f_{m+1}^i + [\theta g_{m+1}^{i+1} + (1-\theta) g_{m+1}^i] \Delta t \end{bmatrix} \right\} + \phi \int_i^{t_{i+1}} q \, \mathrm{d}t \Big|_{\Omega_b} = 0 \tag{13}$$

where the superscripts i and $i+1$ denote values at t_i and t_{i+1}, respectively, θ is a real number between 0 and 1, and $\Delta t = t_{i+1} - t_i$.

Differentiating π expressed in equation (13) with respect to u^{i+1} (a vector including all porewater pressures at nodes) gives

$$\delta\pi = \sum_{\Omega_e} \phi_e^{\mathrm{T}} K \begin{bmatrix} \delta u_m^{i+1} \\ \delta u_{m+1}^{i+1} \end{bmatrix} \tag{14}$$

where

$$K_e = \frac{k\theta\Delta t}{\gamma_w h_e} \begin{bmatrix} 1 & -1 \\ -1 & 1 \end{bmatrix} - \frac{h_e}{2} \begin{bmatrix} \dfrac{\partial (f_m^{i+1} + \theta \Delta t g_m^{i+1})}{\partial u_m^{i+1}} & 0 \\ 0 & \dfrac{\partial (f_{m+1}^{i+1} + \theta \Delta t g_{m+1}^{i+1})}{\partial u_{m+1}^{i+1}} \end{bmatrix} \tag{15}$$

Therefore, the discretized equation (13) can be approximated as

$$\sum_{\Omega_e} \phi_e^{\mathrm{T}} \left(K_e \begin{bmatrix} \delta u_m^{i+1} \\ \delta u_{m+1}^{i+1} \end{bmatrix} - R_e \right) + \phi \int_i^{t_{i+1}} q \, \mathrm{d}t \Big|_{\Omega_b} = 0 \tag{16}$$

where

$$R_e = \frac{k\Delta t}{\gamma_w h_e} \begin{bmatrix} -1 & 1 \\ 1 & -1 \end{bmatrix} [\theta u_e^{i+1} + (1-\theta) u_e^i] + \frac{h_e}{2} \begin{bmatrix} f_m^{i+1} - f_m^i + [\theta g_m^{i+1} + (1-\theta) g_m^i] \Delta t \\ f_{m+1}^{i+1} - f_{m+1}^i + [\theta g_{m+1}^{i+1} + (1-\theta) g_{m+1}^i] \Delta t \end{bmatrix}$$

Following the standard finite element assembly procedure, a symmetrically tri-diagonal set of equations can be derived. This Newton form of iteration (or modified Newton form) for the non-linear equation system converges very rapidly. Generally several iterations will produce very high accuracy.

The element stiffness matrix for equations (3)–(5) is straightforward. We only derive the element stiffness matrix for equation (6) here. Integrating equation (2) gives

$$(\varepsilon - f)^{i+1} = (\varepsilon - f)^i + [\theta' g^{i+1} + (1-\theta') g^i] \Delta t \tag{17}$$

where θ' is a real number between 0 and 1. The θ' has the same meaning as θ' in equation (13), but may have a different value.

Differentiating equation (17) and $g^{i+1} = g(\sigma'^{i+1}, \varepsilon^{i+1})$ with respect to σ'^{i+1} gives

$$\frac{\partial \varepsilon^{i+1}}{\partial \sigma'^{i+1}} = \left(\frac{\partial f}{\partial \sigma'} \right)^{i+1} + \theta' \Delta t \frac{\partial g^{i+1}}{\partial \sigma'^{i+1}} \tag{18}$$

and

$$\frac{\partial g^{i+1}}{\partial \sigma'^{i+1}} = \left(\frac{\partial g}{\partial \sigma'}\right)^{i+1} + \left(\frac{\partial g}{\partial \varepsilon}\right)^{i+1} \frac{\partial \varepsilon^{i+1}}{\partial \sigma'^{i+1}} \tag{19}$$

Substituting equation (18) into equation (19) gives

$$\frac{\partial g^{i+1}}{\partial \sigma'^{i+1}} = \left(\frac{\dfrac{\partial g}{\partial \sigma'} + \dfrac{\partial g}{\partial \varepsilon}\dfrac{\partial f}{\partial \sigma'}}{1 - \theta' \Delta t \dfrac{\partial g}{\partial \varepsilon}} \right)^{i+1} \tag{20}$$

Substituting equation (20) into equation (15) gives

$$K_e = \frac{k\theta\Delta t}{\gamma_w h_e} \begin{bmatrix} 1 & -1 \\ -1 & 1 \end{bmatrix} + \frac{h_e}{2} \begin{bmatrix} \left(\dfrac{\dfrac{\partial f}{\partial \sigma'} + \dfrac{\partial g}{\partial \sigma'}\theta\Delta t + (\theta - \theta')\Delta t \dfrac{\partial g}{\partial \varepsilon}\dfrac{\partial f}{\partial \sigma'}}{1 - \theta' \Delta \dfrac{\partial g}{\partial \varepsilon}} \right)_m^{i+1} & 0 \\ 0 & \left(\dfrac{\dfrac{\partial f}{\partial \sigma'} + \dfrac{\partial g}{\partial \sigma'}\theta\Delta t + (\theta - \theta')\Delta t \dfrac{\partial g}{\partial \varepsilon}\dfrac{\partial f}{\partial \sigma'}}{1 - \theta' \Delta \dfrac{\partial g}{\partial \varepsilon}} \right)_{m+1}^{i+1} \end{bmatrix} \tag{21}$$

Equation (21) is the element stiffness matrix for constitutive equations of the form of equation (2), and it may be adjusted for unloading for some models. For equation (6), the element stiffness matrix becomes

$$K_e = \frac{k\theta\Delta t}{\gamma_w h_e} \begin{bmatrix} 1 & -1 \\ -1 & 1 \end{bmatrix} + \frac{h_e}{2} \begin{bmatrix} \left(\dfrac{\dfrac{\kappa}{V}\dfrac{\psi}{V} + \dfrac{\lambda\theta + (\theta' - \theta)\kappa}{V} g\Delta t}{\sigma' \left(\dfrac{\kappa}{V} + \theta' g \Delta t \right)} \right)_m^{i+1} & 0 \\ 0 & \left(\dfrac{\dfrac{\kappa}{V}\dfrac{\psi}{V} + \dfrac{\lambda\theta + (\theta' - \theta)\kappa}{V} g\Delta t}{\sigma' \left(\dfrac{\kappa}{V} + \theta' g \Delta t \right)} \right)_{m+1}^{i+1} \end{bmatrix} \tag{22}$$

The positiveness of the stiffness matrix is obvious.

From equation (17), we also obtain

$$d\varepsilon^{i+1} = \frac{(\varepsilon - f)^i + [\theta' g^{i+1} + (1-\theta')g^{i+1}]\,\Delta t - (\varepsilon - f)^{i+1}}{1 - \theta'(\partial g/\partial \varepsilon)^{i+1}} \tag{23}$$

The above formulae provide a complete routine for a Newton (or modified Newton) type solution of 1-D consolidation problem.

ANALYSIS OF A CLAY CONSOLIDATION TEST

The FE formulation presented above has been encoded in a finite element program. As an illustration of the solution and its reliability, it has been used to analyse a number of consolidation problems including those problems with closed-form solutions or measured results. One of these problems with measure the results is a 1-D consolidation test with large thickness, that is, Test No. H4 published by Berre and Iversen.[26] This consolidation test was simulated by Garlanger[14] and Yin Graham[16] using finite difference method under constant loading condition.

The soil profile and location of three piezometer points of Test No. H4 are shown in Figure 1. The total initial thickness of Test No. H4 was 0·45 m (0·15 m for each of the three segments S1, S2 and S3 as shown in Figure 1). The surface of the topmost segment (S1) was freely drained and there was no drainage on the left, right and bottom sides. The left and right sides are rigid boundary (no lateral displacement). Displacement and porewater flow are all in the vertical direction (1-D staining problem). Porewater pressures were measured at the bottom of each segment, that is, at points B, C, and D in Figure 1. Average strains were measured for each segment.

The 1-D EVP model in equation (6) is used in the FE analysis of the consolidation of Test No. H4. All the material parameters used in FE modelling are listed in Table I. These parameters have been determined by using a different test on the same clay and published by Yin and Graham.[1,2] The details are not repeated here.

Figure 2(a) illustrates the calculated and measured pore water pressures using the EVP model under a two-step loading (from 53·4 to 89·2 kPa for the first step and from 89·2 to 134·7 kPa for

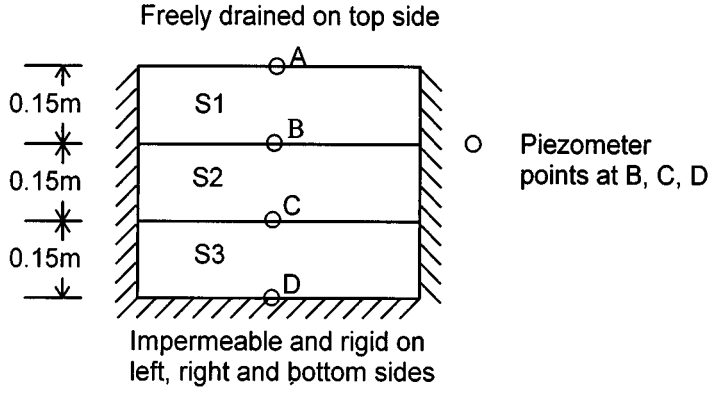

Figure 1. Soil profile and piezometer arrangement for Test No. H4 (after Berre and Iversen[26])

Table I. Soil parameters for modelling consolidation Test no. N4[16]

k (m/min)	κ/V	λ/V	σ'_0 (kPa)	ψ/V	t_0 (min)
$1{\cdot}0 \times 10^{-7}$	0·004	0·158	79·2	0·007	40

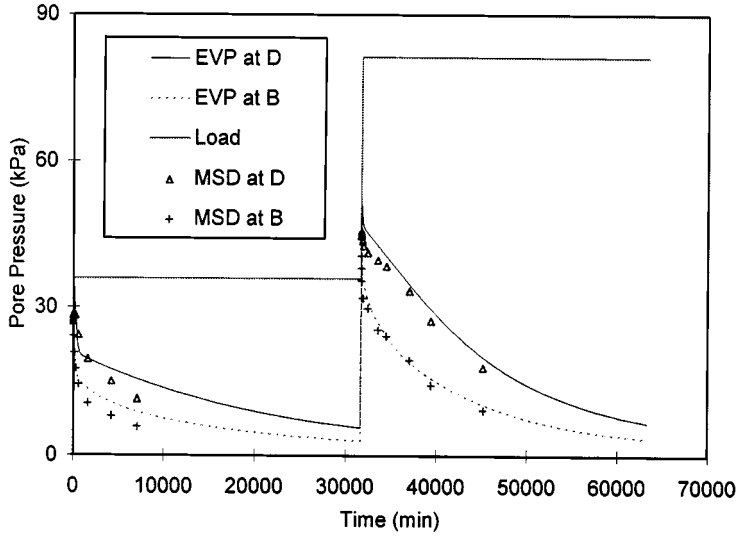

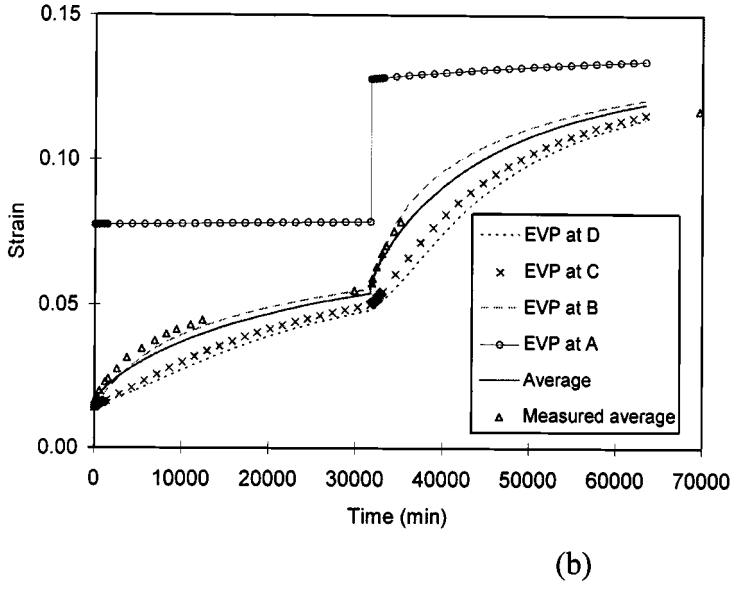

Figure 2. (a) Measured (MSD) and calculated (EVP) porewater pressure and (b) measured (MSD) and calculated (EVP) strain for consolidation Test No. H4 (test data from Berre and Iversen[26])

the second step). Figure 2(b) shows the calculated and measured strains. As can be observed, the computed and measured results are in good agreement.

CONSOLIDATION MODELLING OF CLAY LAYERS AND PARAMETRIC STUDY

This section presents finite element modelling results of the consolidation behaviour of three clay layers under vertical loading with linear increase first then remaining constant. The main features of the FE modelling results are discussed. There are two creep related parameters ψ/V and t_0, in the 1-D EVP model proposed by Yin and Graham.[1,2] The influence of the two parameters on the deformation behaviour and excess porewater pressure dissipation are examined in this section.

A number of FE consolidation modelling case studies, here called numerical tests (i.e. Test No. 1 to Test No. 14), are carried out using the proposed finite element formulation. Figure 3 shows a typical soil profile and related initial stress (solid line) used in the numerical tests. There are three soil layers. The upper layer is 2 m thick, and is of low compressibility. This layer (Clay layer 1) is assumed to obey the non-linear elastic (NLE) model in equation (4). The middle layer (Clay layer 2) and bottom layer (Clay layer 3) are 5·8 m thick each. The compressibility is high for Clay layer 2, and is medial for Clay layer 3. These two layers are assumed to follow the EVP model in equation (6). The NLE model is also employed for Clay layer 2 and Clay layer 3 for comparison with the results obtained by using the EVP model. Table II lists main parameters and variations adopted in the numerical tests. The parameters for Test No. 1 for Clay layer 2 are those in Table 1 and are used as a set of reference parameters.

The 1-D EVP model is dependent on the stress/strain state. For different stress/strain state, the creep rate is different. For example, the creep rate is an 'over-consolidated' range is smaller than the rate in 'normally consolidated' range. The EVP model in equation (6) is a general constitutive equation for modelling the time-dependent stress-strain behaviour under any static loading

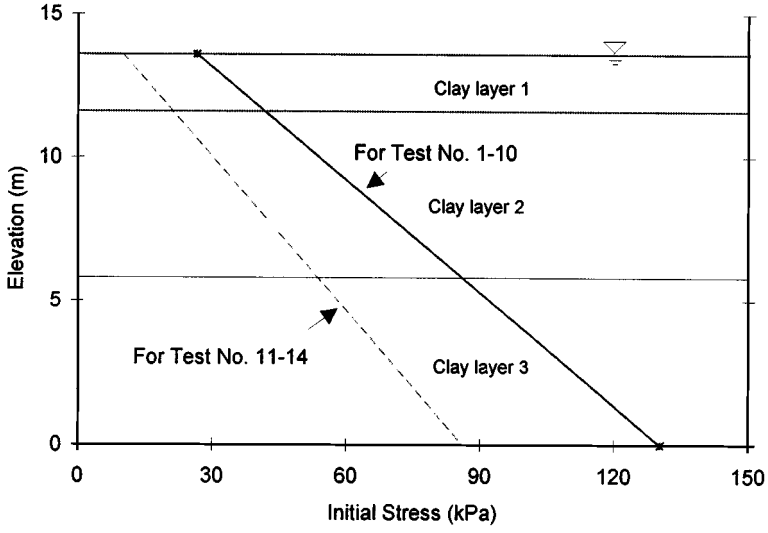

Figure 3. Soil profile and initial stress condition

Table II. Main model parameters and variations in numerical tests

Numerical test no.	Clay layer 1	Clay layer 2	Clay layer 3
1	NLE parameters $k = 1{\cdot}44 \times 10^{-3}$ m/day $a = 0{\cdot}01$	EVP parameters $k = 1{\cdot}44 \times 10^{-4}$ m/day $\kappa/V = 0{\cdot}004$, $\lambda/V = 0{\cdot}158$, $\psi/V = \psi_0/V = 0{\cdot}007$, $\sigma'_0 = 79{\cdot}2$ kPa $t_0 = t^* = 0{\cdot}0278$ day	EVP parameters $k = 1{\cdot}44 \times 10^{-4}$ m/day $\kappa/V = 0{\cdot}004$, $\lambda/V = 0{\cdot}0434$, $\psi/V = \psi_0/V = 0{\cdot}007$, $\sigma'_0 = 86{\cdot}1$ kPa $t_0 = t^* = 0{\cdot}0278$ day
2–4 for 3α values	The same as above	$\psi/V = \alpha \times \psi_0/V$ $\alpha = 1/2, 1/4, 1/10$ others the same above	The same as above
5–8 for 4β values	The same as above	$t_0 = \beta \times t^*$ $\beta = 10,100,1000,10000$ others the same as Test No. 1	The same as above
9	The same as above	NLE parameters $a = 0{\cdot}004$	NLE parameters $a = 0{\cdot}0434$
10	The same as above	NLE parameters $a = 0{\cdot}158$	NLE parameters $a = 0{\cdot}0434$
11–14 for 4α values	Parameters are the same as above, but initial stress is the dashed line in Figure 3	$\psi/V = \alpha \times \psi_0/V$ $\alpha = 1, 1/2, 1/4, 1/10$ others the same as Test no. 1, but initial stress is the dashed line in Figure 3	Parameters are the same as Test No. 1, but initial stress in the dashed line in Figure 3

conditions including unloading/reloading.[1,2] In order to apply the EVP model in consolidation analysis, the initial stress/strain states for the clay layers must be estimated. This makes the consolidation modelling in this paper different from other modelling approaches.

For the initial stress state shown in Figure 3, the corresponding initial strain must be determined. The specimen used for determining the model parameters had an *in situ* effective vertical stress $\sigma'_{\text{in situ}} = 62{\cdot}03$ kPa. The vertical strain under this in-situ stress for this specimen is considered zero according to the EVP model. The clay below this specimen in the field is the same type of clay and shall be and can be modelled by the same EVP model in equation (6). The difference is that the clay below the specimen has a different stress/strain state, normally larger stress (see Figure 3) and larger strain. The reasonable estimation of the initial stress/state for the clay layer are important in the EVP consolidation modelling. This importance is similar to that for the correct estimation of *in situ* stress for an elastic–plastic model, for example, the Cam–Clay model. Many elastic–plastic models are dependent on stresses only so that the initial strains are not required for modelling.

For the FE modelling in this paper, it is assumed that each layer has the same initial 'equivalent time'[1,2] as the specimen tested and used for the calibration of the EVP model. Based on the assumption and the 'equivalent time'[1,2] concept, the initial strains for the clay layer can be

estimated from the following relationships:

For Clay layer 2

$$\varepsilon = 0{\cdot}158 \ln(\sigma'/62{\cdot}03) \tag{24}$$

For Clay layer 3

$$\varepsilon = 0{\cdot}0434 \ln(\sigma'/86{\cdot}1) \tag{25}$$

These strains are the initial strains corresponding to the initial stresses (see the solid line Figure 3) to be used in the 1-D EVP model. The increment $\Delta\varepsilon$ from these initial strains after loading is the true strains for the calculation of compression of the clay layers.

Regarding the boundary conditions in Figure 3, the top of Clay layer 1 is freely drained and the bottom of Clay layer 3 is closed. The load is increased linearly from 0 at day 4–40 kPa at day 242, and remains constant thereafter. For some numerical tests, the water is assumed freely drained at the interface of Clay layer 2 and Clay layer 3.

Figures 4–6 illustrate the isochrones of excess porewater pressure, total effective stress, and the incremental strain $\Delta\varepsilon$ of the soil profile for the case of Test No. 1 with free drainage boundary between Clay layer 2 and Clay layer 3. The free drainage condition between two clay layers may exist in the field where there is a sandy layer between and this sandy layer is connected to the water head on the top of the clay layer under certain geological conditions. It can be seen from Figure 4 that the excess porewater pressure at the bottom of Clay layer 3 firstly increases from 0 to a maximum 40·7 kPa, then decreases with time. As shown in Figure 5, the effective stress at the bottom of Clay layer 3 decreases to a certain extent at the initial stage of loading corresponding to the excess porewater pressure increase as displayed in Figure 4. Figure 6 shows that the vertical strain remains almost unchanged at the same initial stage in which the porewater pressure increases and the effective stress decreases as shown in Figures 4 and 5. With the increase in time, the strain accumulates as porewater pressure decreases. The phenomenon that the excess

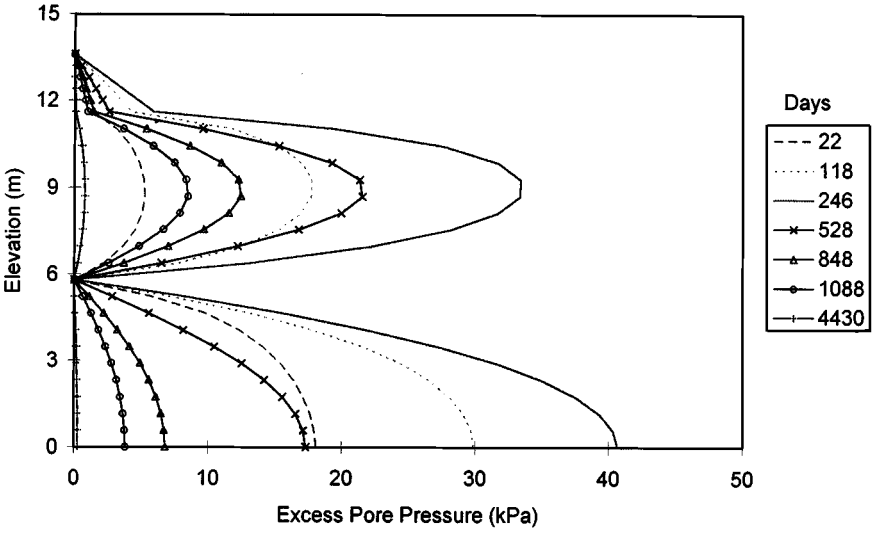

Figure 4. Isochrones of excess porewater pressure for Test No. 1

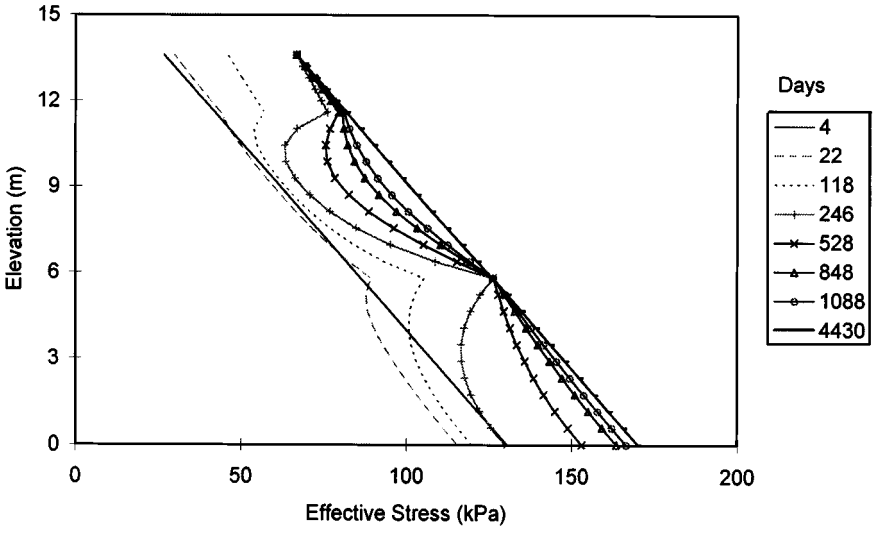

Figure 5. Isochrones of effective stress for Test No. 1

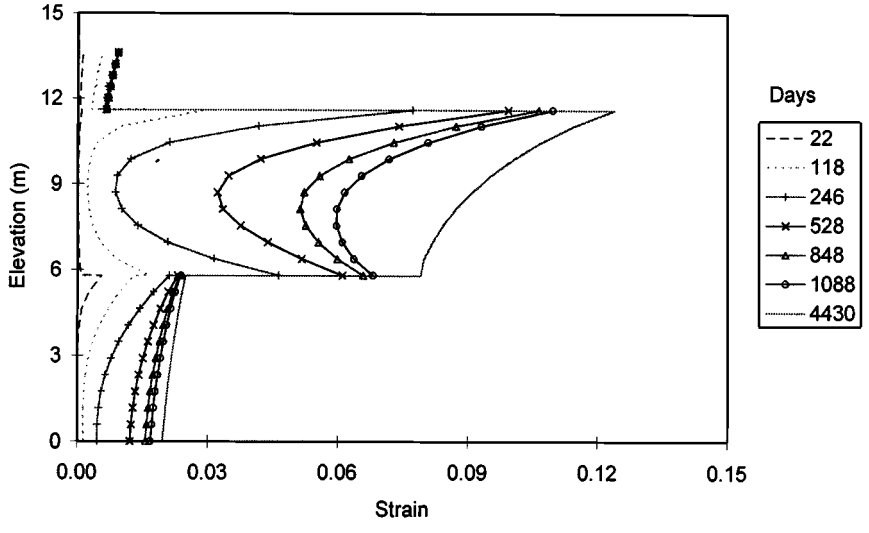

Figure 6. Isochrones of strain $\Delta\varepsilon$ for Test No. 1

porewater pressure at the bottom of Clay layer 3 becomes larger than external loading is due to the creep nature of the clay as explained before by Yin *et al.*[27] The effect of initial stress on deformation behaviour is also clearly demonstrated in Figure 6 from the fact that the strain $\Delta\varepsilon$ decreases with the increase of initial stress in each layer at the final stage.

The influence of ψ/V

For the free drainage condition between Clay layers 2 and 3, changes of parameters in Clay layer 2 will not have any effect on the behaviour of Clay layer 3. Therefore, the consolidation of Clay layer 3 is not discussed for the time being. The influence of the changes of parameters in Clay layer 2 on Clay layer 1 is small due to the high permeability of Clay layer 1. It is obvious, however, that the parameter ψ/V has large influence on the compression, porewater pressure dissipation, and stress/strain state of Clay layer. Figures 7 and 8 demonstrate the effects of the variation of ψ/V ($\alpha = 1, 1/2, 1/4, 1/10$, see Table II) on the compression and porewater pressure changes of Clay layer 2. The numbers after the legend lines in Figures 7 and 8 are numerical test Nos. as listed in Table II. It can be seen from Figure 7 that the compression decreases largely with the decrease of ψ/V. However, the compression-time curves are bound by the two computed curves from Test Nos. 9 and 10 for the elapsed time up to 1100 days. In Tests Nos. 9 and 10, the NLE (non-linear) model in equation (4) is used. In Test No. 9, the parameter a is set to $\kappa/V = 0{\cdot}004$, that is, for the elastic behaviour in the EVP model. In Test No. 10, the parameter a is set to $\lambda/V = 0{\cdot}158$, that is, for the 'elastic–plastic' (or 'reference time' line) behaviour in the EVP model. After 1100 days, the compression time from Test No. 1 is out of the bounds. Figure 8 shows that the porewater pressure dissipates fast with the decrement of ψ/V in the early stage of loading. This phenomenon of fast consolidation was observed during measurement in many embankment constructions.[28] The porewater pressure curves are also bounded by the two curves from Tests Nos. 9 and 10 for the elapsed time up to 1100 days. After this period, the difference in porewater pressures is small and may be negligible

The influence of t_0

The influence of t_0 on the behaviour of Clay layer 2 is similar to ψ/V. Figures 9 and 10 show the effect of the variation of t_0 ($\beta = 1, 10, 100, 1000, 10{,}000$, see Table II) on compression and

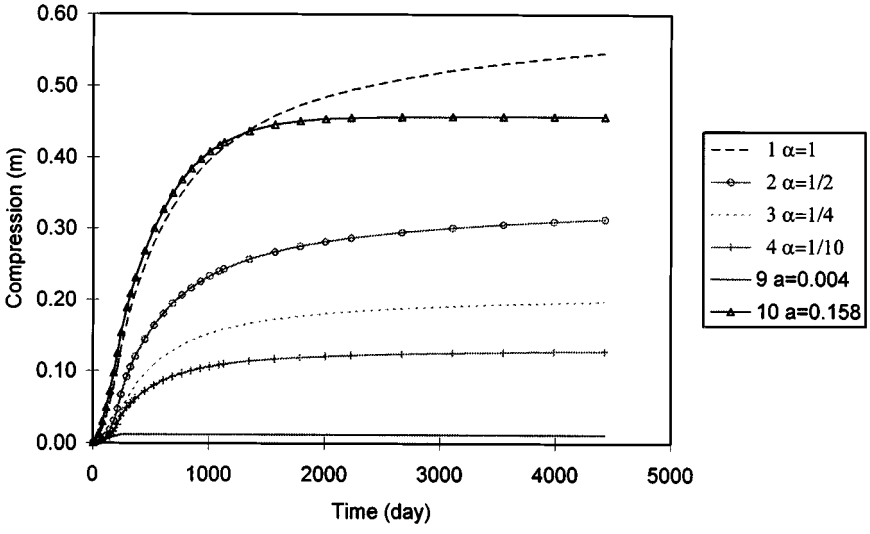

Figure 7. Comparison of Clay layer 2 vs. time for different ψ/V

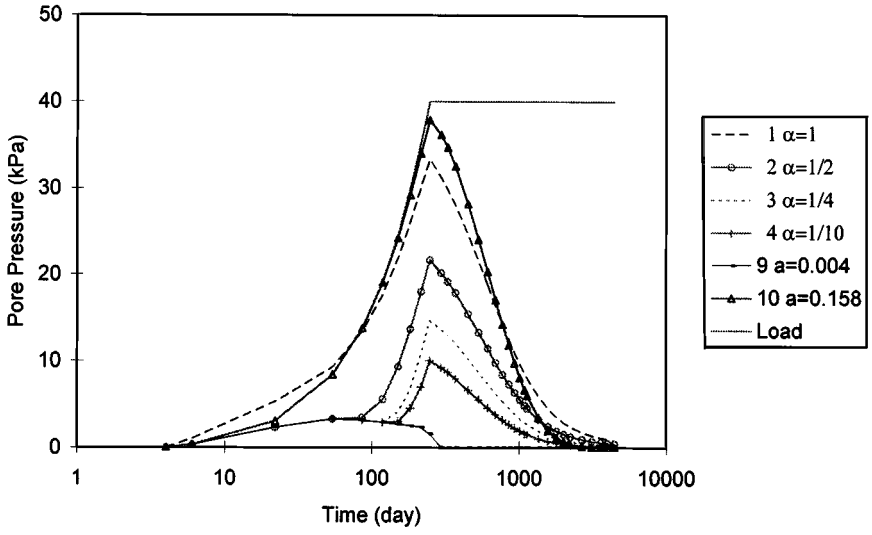

Figure 8. Porewater pressure at the middle of Clay layer 2 vs. time for different ψ/V

porewater pressure of Clay layer 2. As shown in Figure 9, clearly the compression of Clay layer 2 decreases with the increase of t_0, nevertheless the compression-time curves are bounded by the two curves from Tests Nos. 9 and 10 using a non-linear model before day 1100. Figure 10 illustrates that porewater pressure dissipates fast with the increase of t_0 in the early stage of loading. The porewater pressure curves are still limited by the two curves from Tests Nos. 9 and

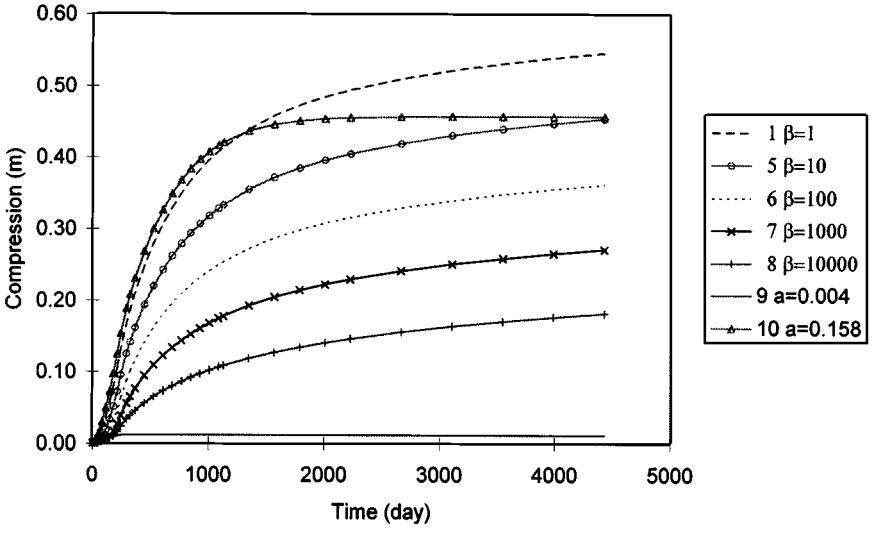

Figure 9. Compression of Clay layer 2 vs. time for different t_0

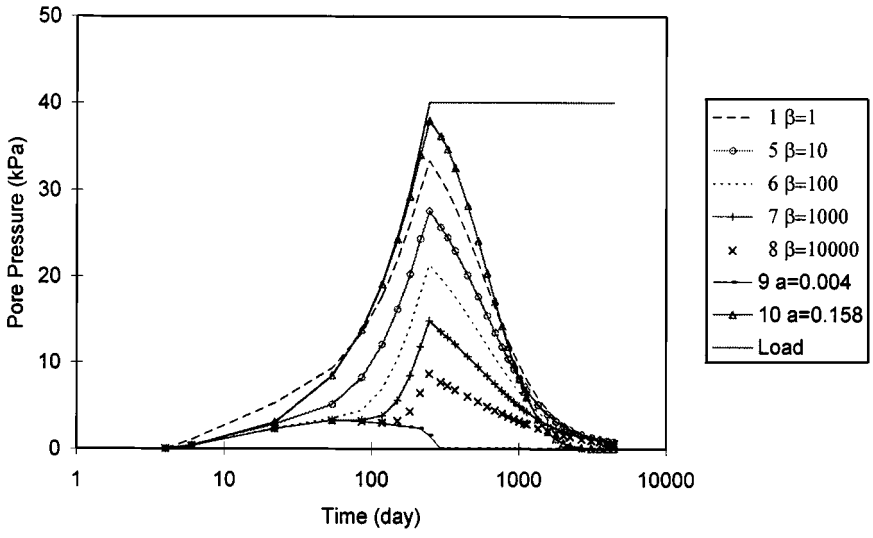

Figure 10. Porewater pressure of Clay layer 2 vs. time for different t_0

10 for most of the time before day 1100. The parameter t_0 is related to the position of the 'reference time' line and should be determined from the test data.[1,2]

The influence of boundary condition

The boundary condition must have a definite influence on the consolidation behaviour of soils without saying. Here we focus on the influence of an internal drainage condition on the consolidation behaviour of different clay layers. In the previous calculations, a free drainage is assumed at the interface of Clay layers 2 and 3. In the following, this condition is cancelled. Figures 11 and 12 exhibit the compression-time and porewater pressure–time curves for different ψ/V (through the variation of $\alpha = 1, 1/2, 1/4, 1/10$) for Clay layer 2. It is clear that the compression becomes slower compared to the curves in Figure 7. And there is a small porewater pressure increase in the initial loading stage due to the change of drainage condition. Figures 13 and 14 show the influence of ψ/V of Clay layer 2 on the compression and porewater pressure of Clay layer 3. As can be seen in the figures, the parameter ψ/V of Clay layer 2 has some effects on Clay layer 3. These effects are due to the different consolidation rates for different ψ/V in Clay layer 2.

The influence of initial stress/strain state

Initial stress exists in almost all geotechnical structures. As discussed early, the 1-D EVP model is dependent on the stress/strain state. In this section, the influence of the initial stress/strain state on the consolidation behaviour of clays is investigated. Figures 15 and 16 show the calculated compression and porewater pressure of Clay layer 2 for two different initial stress/strain states. The first stress/strain state has the initial stress represented by the 'solid line' in Figure 3 and the second has the initial stress represented by the 'dashed line' in Figure 3. The corresponding initial

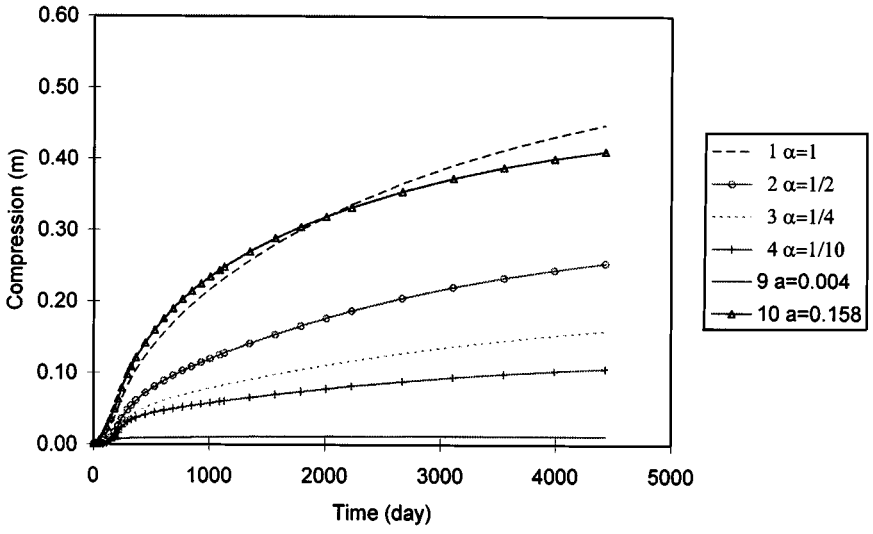

Figure 11. Compression of Clay layer 2 vs. time for different ψ/V if the free drainage at the interface of Clay layers 2 and 3 is cancelled

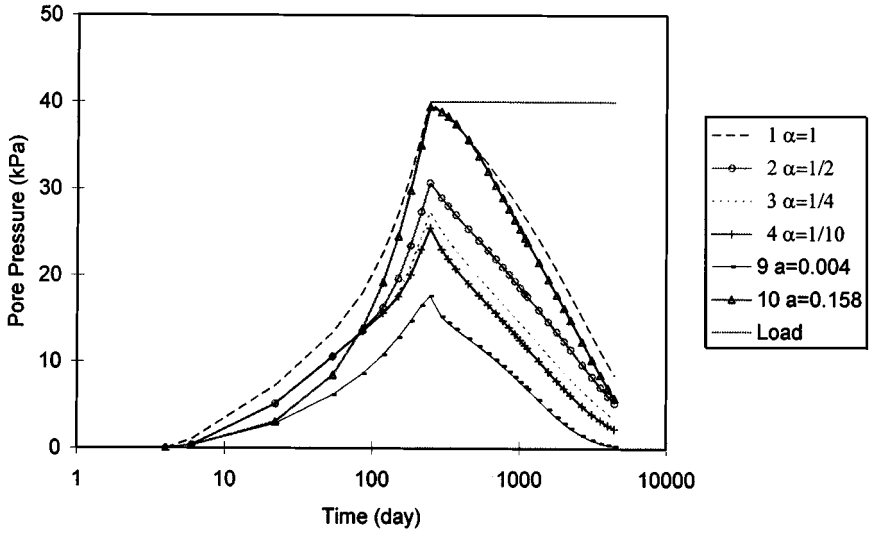

Figure 12. Porewater pressure at the middle of Clay layer 2 vs. time for different ψ/V if the free drainage at the interface of Clay layers 2 and 3 is cancelled

strains for the two cases of initial stresses are calculated by the same equations (23) and (24). In the FE modelling, water is freely drained at the interface of Clay layers 2 and 3. The computed curves of data points with a solid line or a dashed line in Figures 15 and 16 are the FE modelling results using the 'solid line' initial stress or the 'dashed line' initial stress in Figure 3. It can be seen that,

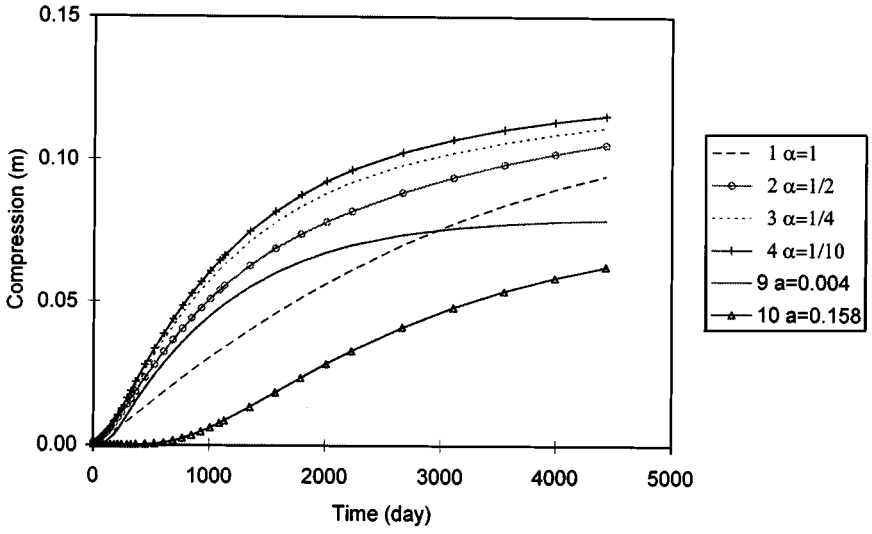

Figure 13. Compression of Clay layer 3 vs. time for different ψ/V if the free drainage at the interface of Clay layers 2 and 3 is cancelled

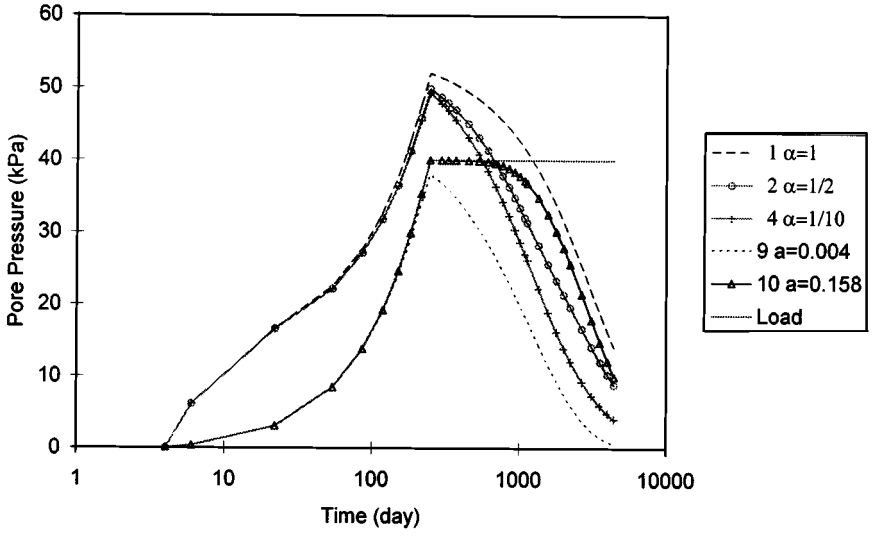

Figure 14. Porewater pressure at the middle of Clay layer 3 vs. time for different ψ/V if the free drainage at the interface of Clay layers 2 and 3 is cancelled

initial stress/strain has a large influence on compression. The compression becomes quite large with the reduction of initial stress for different ψ/V. The porewater pressure also increases with the decrease of initial stress for different ψ/V. The explanation is that the smaller the initial stress, the more the compression for the same creep rate. In turn, porewater pressure is induced.

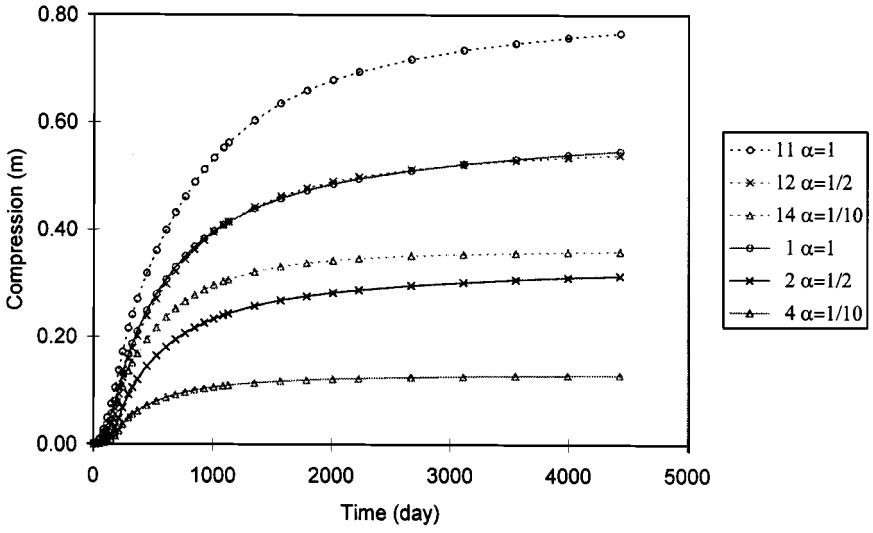

Figure 15. Compression of Clay layer 2 vs. time for different ψ/V and initial stresses (points with solid lines or dashed lines refer to the solid line or dashed line of *in situ* stresses in Figure 3)

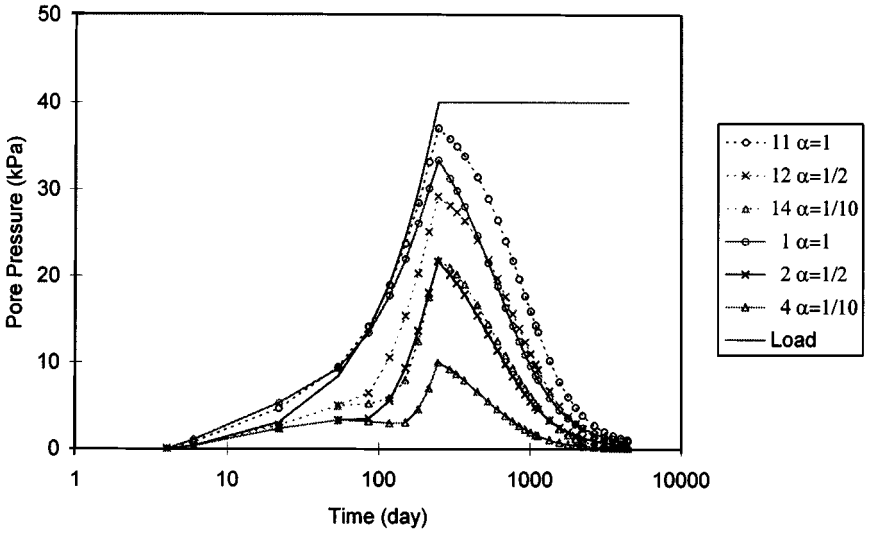

Figure 16. Porewater pressure at the middle of Clay layer 2 vs. time for different ψ/V and initial stress (points with solid lines or dashed lines refer to the solid line or dashed line of *in situ* stresses in Figure 3)

SUMMARY AND CONCLUSIONS

A general 1-D finite element procedure for different constitutive models with an emphasis on the implementation of a highly non-linear elastic visco-plastic model for clays is derived and presented in this paper. In formulating the 1-D finite element procedure, a trapezoidal formula is

used to avoid the unsymmetry of the stiffness matrix for a Newton (modified Newton) iteration scheme. The proposed procedure is then used for consolidation modelling of a consolidation test under staged loading and three-layered clays under continuous loading. The modelling results for the consolidation test are in good agreement with the measured results. A parametric study is carried to investigate the influence of two creep parameters, middle layer drainage condition, and the initial stress/strain state on the compression and porewater pressure dissipation of the three-layered clays. The following conclusions can be drawn.

(a) The proposed FE procedure is efficient for the consolidation modelling using a highly non-linear EVP model and other non-linear models.
(b) The proposed FE model and program can be used to compute the compression and porewater pressure dissipation of multi-layered soils using different soil models under various vertical pressure loading.
(c) The two creep parameters ψ/V and t_0 have significant influence on the compression and porewater pressure dissipation. The larger the ψ/V-values, the more compression and porewater pressure built-up. The influence of t_0 is approximately opposite to that of ψ/V.
(d) The middle layer drainage (free or closed) affects on the compression of clay layers. Without the middle free drainage, the variation of the material parameters of one layer may change the consolidation behaviour of another layer.
(e) The initial stress/strain state has influence on the compression and porewater pressure dissipation of the clay layer for the time-dependent non-linear stress–strain models.

ACKNOWLEDGEMENT

Financial support from The Hong Kong Polytechnic University and Research Grants Council of UGC (Grant No. pdyU 63/96E) of Hong Kong SAR Government of China is gratefully acknowledged.

REFERENCES

1. J. H. Yin and J. Graham, 'Viscous elastic plastic modelling of one-dimensional time dependent behaviour of clays', *Can. Geotech. J.*, **26,** 199–209 (1989).
2. J. H. Yin and J. Graham, 'Equivalent times and elastic visco-plastic modelling of time-dependent stress–strain behaviour of clays', *Canadian Geotechnical J.*, **31,** 42–52 (1994).
3. K. Terzaghi, *Theoretical Soil Mechanics*, Wiley, New York, 1943.
4. M. A. Biot, 'General theory of three-dimensional consolidation', *J. Appl. Phys.*, **12,** 155–164 (1941).
5. A. N. Schofield and C. P. Wroth, *Critical State Soil Mechanics*, McGraw-Hill, London, UK, 1968.
6. L. Bjerrum, 'Seventh Rankine lecture, Engineering geology of Norweigian normally consolidated marine clays as related to settlement of buildings', *Geotechnique*, **17**(2)**,** 81–118 (1967).
7. Y. F. Dafalias, 'Bounding surface elastoplasticity viscoplasticity for particulate cohesive media', in P. A. Vermeer and H. J. Luger, (eds), *IUTAM Symp. on Deformation and Failure of Granular Materials.* Balkema, Rotterdam, 1982, pp. 97–107.
8. T. Adachi and F. Oka, 'Constitutive equations for normally consolidated clay based on elasto-viscoplasticity', *Soils & Foundations*, **22**(4)**,** 57–70 (1982).
9. S. Leroueil, M. Kabbaj, F. Tavenas and R. Bouchard, 'Stress–strain–strain rate relationship for the compressibility of sensitive natural clays', *Geotechnique*, **35**(2)**,** 159–180 (1985).
10. T. Adachi, F. Oka and M. Mimura, 'Mathematical structure of an overstress elastic-viscoplastic model for clay', *Soils & Foundations*, **27**(3)**,** 31–42 (1987).
11. S. Leroueil, M. Kabbaj, and F. Tavenas, Study of the validity of a σ'_v–ε_v–ε_v model in *in situ* conditions', *Soils & Foundations*, **23**(3)**,** 13–25 (1988).
12. R. L. Schiffman and S. K. Arya, 'One-dimensional consolidation', in C. S. Desai and J. T. Christian (eds), *Numerical Methods in Geotechnical Engineering.* McGraw-Hill, New York, 1977, pp. 364–398.
13. C. S. Desai, T. Kuppusamy, D. C. Koutsoftas and R. Janardhanamm, 'A one-dimensional finite element procedure for nonlinear consolidation', *Proc. 3rd Int. Conf. Num. Meth. in Geomech.*, 1979, pp. 143–148.

14. J. E. Garlanger, 'The consolidation of soils exhibiting creep under constant effective stress', *Geotechnique*, **22**(1)**,** 71–78 (1972).
15. M. Kabbaj, F. Oka, S. Leroueil and F. Tavenas, 'Consolidation of natural clays and laboratory testing', in R. N. Young and F. C. Townsend (eds), *Consolidation of Soils*: *Testing and Evaluation*, ASTM STP 892, ASTM, 1986, pp. 378–404.
16. J. H. Yin and J. Graham, 'Elastic visco-plastic modelling of one dimensional consolidation', *Geotechnique*, **46**(3)**,** 515–527 (1996).
17. T. Adachi, F. Oka and M. Mimura, 'Flow analysis of clay layer due to berth construction', *Proc. 6th Int. Conf. Num. Meth. Geomech*., 1988, pp. 697–704.
18. C. C. Ladd, R. Foott, K. Ishihara, F. Schlosser and H. J. Poulos, 'Stress-deformation and strength characteristics', *Proc. 9th Int. Conf. Soil Mech. Found. Eng*., Tokyo, 1977, pp. 421–494.
19. G. Mesri and Y. K. Choi, 'The uniqueness of the end-of-primary void ratio-effective stress relationship', *Proc. 11th. Int. Conf. on Soil Mechanics and Foundation Engineering*, San Francisco, CA, Vol. 2, 1985, pp. 587–590.
20. R. S. Sandhu and E. L. Wilson, 'Finite element analysis of seepage in elastic medium', *J. Eng. Mech. Div. ASCE*, **95,** 641–651 (1969).
21. R. W. Lewis, G. K. Roberts and O. C. Zienkiewics, 'A nonlinear flow and deformation analysis of consolidated problems', *Proc. 2nd Int. Conf. Num. Meth. in Geomech*., 1976, pp. 1106–1118.
22. H. J. Siriwardane and C. S. Desai, 'Two numerical schemes for nonlinear consolidation', *Int. J. Numer. Meth. Eng*., **17,** 405–426 (1981).
23. T. Adachi, F. Oka and Y. Tange, 'Finite element analysis of 2D consolidation using an elasto-viscoplastic consolidation equation', *Proc. 4th Int. Conf. Num. Meth. Geomech*., 1982, pp. 287–296.
24. H. R. Thomas and H. M. Harb, 'Analysis of normal consolidation of viscous clay', *J. Engng. Mech. Div. ASCE*, **116,** 2035–2052 (1990).
25. B. O. Hardin, '1-D strain in normally consolidated cohesive soils', *J. Geotech. Engng. ASCE*, **115**(5)**,** 689–710 (1989).
26. T. Berre and K. Iversen, 'Oedometer tests with different specimen heights on a clay exhibiting large secondary compression', *Geotechnique*, **22**(1)**,** 53–70 (1972).
27. J. H. Yin, J. Graham, J. I. Clark and L. Gao, 'Modelling unanticipated porewater pressures in soft clays', *Canadian Geotechnical J*., **31,** 773–778 (1994).
28. S. Leroueil, F. Tavenas *et al*., 'Construction pore pressures in clay foundations under embankments. Part I: the Saint-Alban test fills', *Can. Geotech. J*., **15,** 54–65 (1978).
29. R. L. Gibson, R. L. Schiffman and R. V. Whitman, 'On two definitions of excess pore water pressure', *Geotechnique*, **39**(1)**,** 169–171 (1989).

